

Moments of Uniform Random Multigraphs with Fixed Degree Sequences*

Philip S. Chodrow†

Abstract. We study the expected adjacency matrix of a uniformly random multigraph with fixed degree sequence \mathbf{d} . This matrix arises in a variety of analyses of networked data sets, including modularity-maximization and mean-field theories of spreading processes. Its structure is well-understood for large, sparse, simple graphs: the expected number of edges between nodes i and j is roughly $\frac{d_i d_j}{\sum_\ell d_\ell}$. Many network data sets are neither large, sparse, nor simple, and in these cases the approximation no longer applies. We derive a novel estimator using a dynamical approach: the estimator emerges from the stationarity conditions of a class of Markov Chain Monte Carlo algorithms for graph sampling. Nonasymptotic error bounds are available under mild assumptions, and the estimator can be computed efficiently. We test the estimator on a small network, finding that it enjoys relative bias against ground truth a full order of magnitude smaller than the standard expression. We then compare modularity maximization techniques using both the standard and novel estimator, finding that the behavior of algorithms depends significantly on the estimator choice. Our results emphasize the importance of using carefully specified random graph models in data scientific applications.

Key words. Random graphs, social networks, Markov Chain Monte Carlo, community structure, estimation

AMS subject classifications. 05C80, 05C82, 91D30, 62-07, 65C05

1. Introduction. The language of graphs offers a standard formalism for representing systems of interrelated objects or agents. Simple graphs model agents connected by a single relation, such as acquaintanceship, proximity, or similarity. In many data sets, however, agents are linked by multiple discrete interactions between i and j . Two agents in a contact network may be in spatial proximity multiple times in the study period. Two agents in a communication network may exchange many emails over the course of a week. In an academic collaboration network, the same two authors may be jointly involved in tens or even hundreds of papers. In such cases, it is natural to draw a distinct edge corresponding to each interaction event, resulting in a multigraph.

A fundamental tool in network data science is null model comparison, which allows the analyst to evaluate whether a feature observed in a given network is surprising when compared to benchmark expectations. When constructing null models of networks, it is common to fix the degree sequence \mathbf{d} of the data, which encodes the number of interactions for each node and is known to constrain many of a network’s macroscopic properties [29]. Applying this principle to multigraphs yields the following standard formulation. Let $\mathcal{G}_{\mathbf{d}}$ be the set of all multigraphs with degree sequence \mathbf{d} . The maximum-entropy null multigraph with specified degree sequence \mathbf{d} is the uniform distribution $\eta_{\mathbf{d}}$ on the space $\mathcal{G}_{\mathbf{d}}$.

In many cases a complete set of samples is not required – only some of its moments. We

*Uploaded September 20, 2019

Funding: PSC acknowledges support from the National Science Foundation under Graduate Research Fellowship Grant 1122374.

†Operations Research Center and Laboratory for Information and Decision Systems, Massachusetts Institute of Technology (pchodrow@mit.edu).

therefore consider a simpler question: if \mathbf{W} is the adjacency matrix of multigraph $G \sim \eta_{\mathbf{d}}$, what is the value of the expected adjacency matrix $\omega = \mathbb{E}[\mathbf{W}]$? The entry ω_{ij} of ω gives the expected number of edges between nodes i and j , and ω thus summarizes the first moments of $\eta_{\mathbf{d}}$. These moments have several important applications in network science. Among these is community-detection via modularity-maximization [28], which in many formulations includes a term for the expected number of edges between nodes under a suitably specified null model. Despite the simplicity of the problem and relevance of the answer, this problem has received relatively little mathematical attention.

Before surveying existing approaches to this problem, we first fix notation. Throughout, $\mathcal{G}_{\mathbf{d}}$ refers to the set of multigraphs without self-loops. From a modeling perspective reflects an assumption that agents do not meaningfully interact with themselves. An element $G \in \mathcal{G}_{\mathbf{d}}$ has a fixed number n of nodes and $m = \frac{1}{2} \sum_i d_i$ of edges. The vector of ones is denoted \mathbf{e} , and its dimension will be specified by context. We use bold symbols to denote matrices and vectors, and standard symbols to denote scalars; thus, $\mathbf{w} = [w_{ij}]$ enumerates the elements of matrix \mathbf{w} . Capital letters refer to random objects, while lowercase letters refer to fixed ones; thus, $\mathbf{W} = \mathbf{w}$ states that random matrix \mathbf{W} takes a fixed value \mathbf{w} . We use Greek letters to denote expectations of random objects – for example, $\omega = \mathbb{E}[\mathbf{W}]$. A statistical estimator of a quantity is distinguished by a hat. For example, the equation $\mathbb{E}[\hat{\Omega}] = \omega$ states that $\hat{\Omega}$ is an unbiased estimator of ω .

One approach to estimating ω is Monte Carlo sampling. We sample s independent and identically-distributed samples $W^{(1)}, \dots, W^{(s)} \sim \eta_{\mathbf{d}}$, and construct the estimator

$$\hat{\Omega}^{\text{mc}}(\mathbf{d}) = \frac{1}{s} \sum_{\ell=1}^s \mathbf{W}^{(\ell)}.$$

The estimator $\hat{\Omega}^{\text{mc}}$ is a random function of \mathbf{d} , parameterized by the sample size s . The Strong Law of Large Numbers ensures that $\hat{\Omega}^{\text{mc}} \rightarrow \omega$ almost surely as the number of samples s grows large. Stronger results are possible: since each entry W_{ij} is bounded, the variance σ_{ij}^2 of W_{ij} is finite and we can apply the Central Limit Theorem to provide quantitative bounds on the convergence rate. This attractive picture is marred by a computational inconvenience: the size and complex combinatorial structure of $\mathcal{G}_{\mathbf{d}}$ makes exact sampling intractable. Markov Chain Monte Carlo (MCMC) methods [18] are therefore required. Even here, there are few known mixing time bounds on MCMC samplers for this space. The available results [19, 20] are not encouraging, and there are heuristic reasons to believe that there are limits on our ability to improve them.

An alternative estimator $\hat{\omega}^0$, extremely common in the network science literature, is defined entrywise by

$$(1.1) \quad \hat{\omega}_{ij}^0(\mathbf{d}) = \begin{cases} f_{ij}(\mathbf{d}) \triangleq \frac{d_i d_j}{2m} & i \neq j \\ 0 & i = j. \end{cases}$$

Unlike $\hat{\Omega}^{\text{mc}}$, $\hat{\omega}^0$ is a deterministic function of \mathbf{d} that is essentially free to compute. The functional form $f_{ij}(\mathbf{d})$ can be derived in multiple ways. For example, it is the definition of the expected edge density between distinct nodes i and j in the model of Chung and Lu

[11, 12], which preserves \mathbf{d} in expectation rather than deterministically.¹ We will therefore refer to Equation (1.1) as the “CL estimate” after Chung and Lu, though we emphasize that these authors did not use this expression as an estimator for any of the models we consider here, and indeed restricted their attention to graphs without parallel edges. The estimator $\hat{\omega}^0$ was also derived heuristically by Newman and Girvan when they introduced modularity maximization as a method for community detection in networks [28, 26]. In their derivation, we approximate the number of edges between i and j as follows. Node i has d_i edges. Each of these edges must connect to one of the $n - 1$ other nodes. A “random edge” is attached to node j with probability roughly $\frac{d_j}{2m - d_i}$. Assuming that $d_i \ll 2m$ yields $\hat{\omega}_{ij}^0$. It is important to note that this derivation does not formalize any probability measure over a set of graphs. Thus, although $\hat{\omega}^0$ is sometimes described as the expectation of a “random graph with fixed degree sequence,” this is not exactly true for any common models except that of Chung and Lu. In particular, $\hat{\omega}^0$ possesses no guarantees related to its performance as an estimator for the uniform model $\eta_{\mathbf{d}}$. As we will see this performance can indeed be quite poor on data sets with high edge densities.

In this article, we construct an estimator of ω for dense multigraphs that is both scalable and accurate. By treating the MCMC sampler as a stochastic dynamical system whose state space is $\mathcal{G}_{\mathbf{d}}$, we derive stationarity conditions describing the moments of $\eta_{\mathbf{d}}$. As we will show, there exists a vector $\beta \in \mathbb{R}_+^n$ such that

$$\chi_{ij} \triangleq \eta_{\mathbf{d}}(W_{ij} \geq 1) \approx \frac{\beta_i \beta_j}{\sum_i \beta_i} = f_{ij}(\beta)$$

for all $i \neq j$. Furthermore, the first moment of \mathbf{W} under $\eta_{\mathbf{d}}$ is approximately

$$\omega_{ij} \approx \frac{\chi_{ij}}{1 - \chi_{ij}}.$$

Taken together, these two equations provide a method for computing an estimate of ω given knowledge of the vector β . We construct an estimator $\hat{\beta}$ of this vector by solving the system of n equations

$$\sum_j \frac{f_{ij}(\beta)}{1 - f_{ij}(\beta)} = d_i, \quad i = 1, \dots, n.$$

This can be done efficiently by a simple iterative algorithm that calls Newton’s method as a subroutine. Finally, from $\hat{\beta}$ we construct an estimator $\hat{\omega}^1$ of ω . As we show, this estimator is both easier to compute than $\hat{\Omega}^{\text{mc}}$ and much more accurate than $\hat{\omega}^0$. Furthermore, we can view the Chung-Lu estimator $\hat{\omega}^0$ as an approximation of $\hat{\omega}^1$, obtained from the latter via a sequence of two linear approximations.

1.1. Outline. In Section 2, we review two important null multigraph models – the configuration model and the uniform model – as well as a unified MCMC algorithm for sampling from each of them. The analysis of this algorithm forms the heart of our derivation of the

¹In their original model, there is also an expected number $\frac{d_i^2}{2m}$ of self-loops on node i .

estimate $\hat{\omega}^1$ in Section 3. This estimator depends on the unknown vector β , which must be learned from \mathbf{d} . We offer a simple, efficient algorithm for doing so in Section 4. In Section 5 we turn to experiments. We first check the accuracy of $\hat{\omega}^1$ on a subset of a high school contact network. Whereas $\hat{\omega}^0$ is significantly biased on this data set, $\hat{\omega}^1$ is nearly unbiased and decreases the mean relative error of the estimate by an order of magnitude. We then study the behavior of modularity maximization when the standard null expectation $\hat{\omega}^0$ is replaced by $\hat{\omega}^1$. We find that the behavior of a multiway spectral algorithm [37] depends strongly on both the choice of null expectation and the data set under study. We close in Section 6 with a discussion and suggestions for future work.

2. Random Graphs with Fixed Degree Sequences. Our interest will focus on the uniform model $\eta_{\mathbf{d}}$, but it will be useful draw comparisons to the somewhat more commonly-used configuration model [7].

Definition 2.1 (Configurations). For a fixed node set N and degree sequence $\mathbf{d} \in \mathbb{Z}_+^n$, let

$$\Sigma_{\mathbf{d}} = \biguplus_{i=1}^n \{i_1, \dots, i_{d_i}\},$$

where \uplus denotes multiset union. The copies i_1, \dots, i_{d_i} are called stubs of node i . A configuration $C = (N, E)$ consists of the node set N and an edge set $E = \{(i_k, j_k)\}_{k=1}^m$ which partitions $\Sigma_{\mathbf{d}}$ into unordered pairs. An edge of the form $\{i_k, i_\ell\}$ is called a self-loop. The process of forming C from $\Sigma_{\mathbf{d}}$ is often called stub-matching.

Let $\mathcal{C}_{\mathbf{d}} \subset \Sigma_{\mathbf{d}}$ be the set of all configurations with degree sequence \mathbf{d} that do not include any self-loops. There is a natural surjection $g : \mathcal{C}_{\mathbf{d}} \rightarrow \mathcal{G}_{\mathbf{d}}$. The image of C under g is obtained by replacing all stubs with their corresponding nodes and consolidating the result as a multiset. The uniform distribution on $\mathcal{C}_{\mathbf{d}}$ induces a distribution on $\mathcal{G}_{\mathbf{d}}$ via g . Denote by $g^{-1} : \mathcal{G}_{\mathbf{d}} \rightarrow 2^{\mathcal{C}_{\mathbf{d}}}$ the function that assigns to each element of $\mathcal{G}_{\mathbf{d}}$ its preimage in $\mathcal{C}_{\mathbf{d}}$ under g .

Definition 2.2 (Configuration Model). Let $\lambda_{\mathbf{d}}$ be the uniform distribution on $\mathcal{C}_{\mathbf{d}}$. The configuration model on $\mathcal{G}_{\mathbf{d}}$ is the distribution $\mu_{\mathbf{d}} = \lambda_{\mathbf{d}} \circ g^{-1}$.

The distinction between $\eta_{\mathbf{d}}$ and $\mu_{\mathbf{d}}$ – and its implications for data analysis – was recently highlighted by Fosdick et al. [18]. We have diverged from their terminology: our “uniform model” is their “configuration model on non-loopy, vertex-labeled multigraphs” and our “configuration model” is their “configuration model on non-loopy, stub-labeled multigraphs.”

The distinction between uniform and configuration models lies in how they weight graphs with multi-edges. For example, let C_1 and C_2 be two configurations. Suppose that C_1 contains the matchings $(i_1, j_1), (i_2, j_2)$ and C_2 contains the matchings $(i_1, j_2), (j_2, i_1)$, and that they otherwise agree on all other stubs. Let $G = g(C_1) = g(C_2)$. Under the uniform model, G is considered to be a single state. Under the configuration model, on the other hand, the probability mass placed on G reflects both C_1 and C_2 (as well as all other elements of $g^{-1}(G)$). In particular, the configuration model will tend to place higher probabilistic weight on states with large numbers of parallel edges than will the uniform model.

In the absence of parallel edges, the uniform and configuration models are nearly equivalent, in the following sense. Let A be the event that G is simple, without self-loops or parallel edges. Then, it is direct to show (e.g. [7]) that, for all G , $\eta_{\mathbf{d}}(G|A) = \mu_{\mathbf{d}}(G|A)$. The reason

is that, when G is simple, the sizes of the preimages $g^{-1}(G)$ depend only on the degree sequence \mathbf{d} . Since \mathbf{d} is fixed in $\mathcal{G}_{\mathbf{d}}$, these preimages all have the same size. Thus, when a *simple* random graph is required, the uniform model $\eta_{\mathbf{d}}$ and configuration model $\mu_{\mathbf{d}}$ are operationally equivalent. We can sample from $\eta_{\mathbf{d}}(\cdot|A)$ by repeatedly sampling from $\mu_{\mathbf{d}}$ until a simple graph is produced. Furthermore, when the degree sequence \mathbf{d} grows slowly relative to n , $\mu_{\mathbf{d}}(A)$ is bounded away from zero by a function that depends on moments of \mathbf{d} when n grows large [7, 24, 2]. This provides an estimate on the number of samples from $\mu_{\mathbf{d}}$ required to produce a single sample from $\eta_{\mathbf{d}}(\cdot|A)$. The computational importance of this relationship is that stub-matching for sampling from $\mu_{\mathbf{d}}$ is well-understood and often fast.

However, this sampling approach is limited in two important application contexts. For dense graphs, $\mu_{\mathbf{d}}(A)$ may be extremely small, and the number of samples required to produce a simple graph may be prohibitive. While it is possible to make post-hoc edits to the graph to remove self-loops and multiple edges [25, 31], such methods can generate substantial and uncontrolled bias in finite graphs. Second and more importantly for our context, there is no equivalence between the unconditional distributions $\eta_{\mathbf{d}}$ and $\mu_{\mathbf{d}}$ on spaces of multigraphs. Stub-matching cannot therefore be used to sample from $\eta_{\mathbf{d}}$.

2.1. Markov Chain Monte Carlo. An alternative approach to sampling uses Markov chains to explore structured sets of graphs. There exists a large constellation of related algorithms for this class of task, including the sampling of marginal-constrained binary matrices [35, 3]; degree-regular [36, 23, 21] and degree-heterogeneous [9, 34, 5, 13] simple graphs; and graphs with degree-correlation constraints [1]. Most of these algorithms operate by repeatedly swapping edges in such a way as to preserve the required graph structure.

A fairly general variant, formulated by Fosdick et al. [18], can sample from either the uniform model $\eta_{\mathbf{d}}$ or the configuration model $\mu_{\mathbf{d}}$ on $\mathcal{G}_{\mathbf{d}}$. We define an edge swap to be a random function of two edges that share no nodes.² It interchanges a node on the first edge with a node on the second:

$$\text{EdgeSwap}((i, j), (k, \ell)) = \begin{cases} (i, k), (j, \ell) & \text{with probability } 1/2 \\ (i, \ell), (j, k) & \text{with probability } 1/2. \end{cases}$$

An edge swap does not change the total number of edges incident to nodes i , j , k , or ℓ , and therefore preserves \mathbf{d} . Starting from a graph G_0 with the desired degree sequence \mathbf{d} , repeated edge-swaps can therefore be used to obtain a random sequence of elements of $\mathcal{G}_{\mathbf{d}}$. Since each element of this sequence depends stochastically only on its predecessor, the sequence is a Markov chain. We perform Markov Chain Monte Carlo as follows. At each time step, we select two distinct, uniformly random edges (i, j) and (k, ℓ) . We then perform a pairwise edge-swap of these edges with acceptance probability $a((i, j), (k, \ell))$, which is equal to unity for the configuration model and to $(W_{ij}W_{k\ell})^{-1}$ for the uniform model. Otherwise, we record

²Swaps involving edges that intersect are used when sampling from spaces that include self-loops [18].

the current state again and resample. Formally,

Algorithm 1: MCMC Sampling for $\eta_{\mathbf{d}}$ and $\mu_{\mathbf{d}}$

Input: degree sequence \mathbf{d} , initial graph $G_0 \in \mathcal{G}_{\mathbf{d}}$, desired distribution $\rho \in \{\eta_{\mathbf{d}}, \mu_{\mathbf{d}}\}$, sample interval $\delta t \in \mathbb{Z}_+$, sample size $s \in \mathbb{Z}_+$.

- 1 **Initialization:** $t \leftarrow 0, G \leftarrow G_0$
- 2 **for** $t = 1, 2, \dots, s(\delta t)$ **do**
- 3 sample (i, j) and (k, ℓ) uniformly at random from $\binom{E_t}{2}$
- 4 **if** $\text{Uniform}([0, 1]) \leq a((i, j), (k, \ell))$ **then**
- 5 $G_t \leftarrow \text{EdgeSwap}((i, j), (k, \ell))$
- 6 **else**
- 7 $G_t \leftarrow G_{t-1}$

Output: $\{G_t$ such that $t|\delta t\}$

For sufficiently large sample intervals δt , the output of [Algorithm 1](#) will be approximately i.i.d. according to the desired distribution ρ , as guaranteed by the following result.

Theorem 2.3 (Fosdick et al. [18]). *The Markov chain $\{G_t\}$ defined by [Algorithm 1](#) is ergodic and reversible with respect to the input distribution ρ . As consequence, samples $\{G_t\}$ generated by [Algorithm 1](#) are asymptotically independent and identically distributed according to ρ as $\delta t \rightarrow \infty$.*

These results provide a principled solution to the problem of asymptotically exact sampling from $\eta_{\mathbf{d}}$, and can therefore be used to construct an estimator $\hat{\Omega}^{\text{mc}}$ of ω with arbitrary levels of accuracy by letting the sample size s and sample interval δt grow large. There are two performance-related issues when using [Algorithm 1](#) sampling in practice, both of which are connected to the number of edges in the graph. First is the question of how large δt should be to ensure that the samples are sufficiently close to independence. Heuristically, δt should scale with the mixing time of the chain, but very few bounds on mixing times for chains of this type appear to be available. Greenhill and collaborators [20, 19] have derived the only bounds known to this author for edge-swap Markov chains. In the space of simple graphs, under certain regularity conditions on the degree sequence, they provide a mixing time bound with scaling $O(d_*^{14} m^{10} \log m)$, where $d_* = \max_i d_i$. This is not especially reassuring for practical applications. The second issue relates to the acceptance probabilities themselves. In a dense multigraph the number W_{ij} of edges between i and j will typically be large, resulting in low acceptance rates. Indeed, supposing that a typical entry W_{ij} scales approximately linearly with m , the acceptance probabilities would scale as m^{-2} . We therefore conjecture that the overall mixing time of [Algorithm 1](#) for the uniform model on dense multigraphs is no smaller than $O(m^3 \log m)$, though a more precise statement and proof would be welcome. While much better than the best known proven results, even this scaling could likely be prohibitive for many graphs of interest.

These considerations suggest that forming the MCMC estimate $\hat{\Omega}^{\text{mc}}$ may not be a computationally practical way to estimate ω when m is large. Despite these limitations, [Algorithm 1](#) lies at the heart of our main results. We view the algorithm as defining a stochastic dynamical system on the space $\mathcal{G}_{\mathbf{d}}$, and then study the moments of \mathbf{W} at stationarity.

3. A Dynamical Approach to Model Moments. We introduce some additional notation to facilitate the calculation. Brackets $\langle \cdot, \cdot \rangle$ denote the Euclidean inner product. \mathbf{W}_i is the i th row or column of matrix \mathbf{W} ; all matrices we encounter will be symmetric and so no ambiguity will arise. All sums over node indices have implicit limits from 1 to n . Let $z(m) = m(m-1)$. Finally, let $a \wedge b$ and $a \vee b$ denote the pairwise minimum and maximum of scalars a and b , respectively.

Algorithm 1 describes a stochastic dynamical update on the space $\mathcal{G}_{\mathbf{d}}$ of multigraphs, which we identify with the space of symmetric matrices with nonnegative integer entries and zero diagonals. Let $\Delta(t) = \mathbf{W}(t+1) - \mathbf{W}(t)$ be the (random) increment in \mathbf{W} in timestep $t+1$. We implicitly regard \mathbf{W} and Δ as functions of t , suppressing the argument for notational sanity. We can separate $\Delta = \Delta^+ - \Delta^-$, where $\Delta_{ij}^+ = (\Delta_{ij} \vee 0)$ and $\Delta_{ij}^- = (-\Delta_{ij} \vee 0)$. The first term Δ_{ij}^+ describes the (random) number of edges flowing into the pair (i, j) and the second term Δ_{ij}^- the random number of edges flowing out. Conservation of edges implies that $\sum_{ij} \Delta_{ij}^+ = \sum_{ij} \Delta_{ij}^-$. Since a pair of nodes can only gain or lose one edge at a time under the dynamics, the entries Δ_{ij}^+ and Δ_{ij}^- are Bernoulli random variables. These Bernoulli variables are correlated, since at most two entries of each matrix are nonzero in a given timestep. Let $\delta^+ = \mathbb{E}[\Delta^+]$ and $\delta^- = \mathbb{E}[\Delta^-]$.

Two things must hold at stationarity of **Algorithm 1**. First, all moments of \mathbf{W} must be constant in time. Second, since the stationary distribution of **Algorithm 1** is ρ by construction, these moments of \mathbf{W} are the desired moments of ρ . We can therefore approximately compute moments of ρ by approximately solving conveniently chosen stationarity conditions. We therefore study the equations

$$(3.1) \quad \mathbb{E} \left[(W_{ij} + \Delta_{ij})^p - W_{ij}^p \right] = \sum_{s=1}^p \binom{p}{s} \mathbb{E} \left[W_{ij}^{p-s} \Delta_{ij}^s \right] = 0,$$

for positive integers p .

3.1. Illustration: The Configuration Model. We will derive a version of the Chung-Lu estimator $\hat{\omega}^0$ for the configuration model by solving the $p=1$ stationarity condition.

Theorem 3.1. *Under the configuration model $\mu_{\mathbf{d}}$, for all $i \neq j$,*

$$(3.2) \quad \omega_{ij} = \hat{\omega}_{ij}^0 - \frac{\mathbb{E}[\langle \mathbf{W}_i, \mathbf{W}_j \rangle]}{2m}.$$

Proof. We first derive expressions for Δ^- and Δ^+ by stepping through the stages of **Algorithm 1**. For the former, note that $\Delta_{ij}^- = 1$ only if edge (i, j) is sampled in the first stage of the iteration. Sampling occurs without replacement, and the probability that (i, j) and (k, ℓ) are sampled is therefore $\frac{2W_{ij}W_{k\ell}}{z(m)}$. Under stub-labeling, $a((i, j), (k, \ell)) = 1$. Summing across k and ℓ , we obtain

$$\delta_{ij}^- = \mathbb{E} \left[\sum_{k, \ell} \frac{2W_{ij}W_{k\ell}}{z(m)} \right],$$

which after some algebra may be written

$$\delta_{ij}^- = \frac{2}{z(m)} \mathbb{E} [W_{ij} (2m - d_i - d_j + W_{ij})].$$

We can derive a similar expression for δ_{ij}^+ . A new edge (i, j) is generated when two edges of the form (i, k) and (ℓ, j) are selected for swap, which again occurs with probability $\frac{2W_{ik}W_{\ell,j}}{z(m)}$. There is probability $\frac{1}{2}$ that the swap produces new edges $(i, j), (k, \ell)$ and probability $\frac{1}{2}$ that the swap produces edges $(i, \ell), (k, j)$ instead. Consolidating and simplifying, we have

$$\begin{aligned}\delta_{ij}^+ &= \mathbb{E} \left[\frac{1}{z(m)} \sum_{k, \ell \neq i, j} W_{ik} W_{\ell j} \right] \\ &= \frac{1}{z(m)} \mathbb{E} [2(d_i - W_{ij})(d_j - W_{ij}) - \langle \mathbf{W}_i, \mathbf{W}_j \rangle] .\end{aligned}$$

Choosing $p = 1$ in Equation (3.1), we must have $\delta_{ij}^+ = \delta_{ij}^-$ at stationarity. Inserting our derived expressions and simplifying yields the result. \blacksquare

Theorem 3.1 does not give an explicit operational solution for w_{ij} , since the righthand side contains higher moments of \mathbf{W} . Progress can be made in the “large, sparse regime,” in which we assume that n is large and the entries of \mathbf{d} small relative to n . In this case, the expression $\mathbb{E}[\langle \mathbf{W}_i, \mathbf{W}_j \rangle]$, which contains n terms quadratic in the entries of \mathbf{W} , should be dominated by $d_i d_j$, which implicitly contains $\binom{n}{2}$ quadratic terms. The second term should then be much smaller in magnitude than the first, and we thus have $\omega \approx \hat{\omega}^0(\mathbf{d})$. This approximation can be made asymptotically precise by imposing assumptions on the dependence of \mathbf{d} on n . Through analysis of Algorithm 1, we have derived both $\hat{\omega}^0$ and explicit error terms that are often elided in the network science literature.

3.2. Moments of the Uniform Model. The analysis of the uniform model is somewhat more subtle. In the configuration model considered above, many the sums that appeared in the calculation of δ^+ and δ^- were fixed constants. As we will see, this no longer holds in the vertex-labeled model. Because of this, we require an additional assumption on $\eta_{\mathbf{d}}$ in order to make progress.

Define the matrix \mathbf{X} entrywise by $X_{ij} = \mathbb{1}(W_{ij} > 0)$. For convenience, we adopt the convention $0/0 = 0$ under which the identity $W_{ij}/W_{ij} = X_{ij}$ holds even when $W_{ij} = 0$. The matrix \mathbf{X} is interpretable as the adjacency matrix of the simple graph obtained by collapsing all sets of parallel edges into single edges. Let $\mathbf{p} : \mathbb{R}^{n \times n} \rightarrow \mathbb{R}^s$ be 1-Lipschitz, and let $q : \mathbb{R}^s \rightarrow \mathbb{R}$ be nondecreasing. Define u_* as the smallest value of u for which the following holds: for any finite index set $I = (i_1, j_1), \dots,$

$$(3.3) \quad \mathbb{E}[q(\mathbf{p}(\mathbf{X}) - u|I|\mathbf{e})] \leq \mathbb{E}[(q \circ \mathbf{p})(\mathbf{X}) | \mathbf{X}_I = \mathbf{e}] \leq \mathbb{E}[q(\mathbf{p}(\mathbf{X}) + u|I|\mathbf{e})] .$$

Intuitively, u_* bounds the dependence on linear functions of conditioning on events of the form $\{X_{ij} = 1\}$. Conditioning on $|I|$ such events effectively modifies sums of the elements of \mathbf{X} by no more than $u_* |I|$. It is direct to verify that $1 \leq u_* \leq n^2$. It is natural to conjecture that u_* is quite small, and is perhaps even equal to its lower bound. The complex combinatorial structure of $\mathcal{G}_{\mathbf{d}}$ makes it difficult to see a path toward a rigorous proof. For the remainder of this article, we will generally treat u_* as small, although the technical statements of the results do not depend directly on this assumption.

Let $\mathbf{B} = \mathbf{X}\mathbf{e}$ and $Y = \frac{1}{2}\langle \mathbf{e}, \mathbf{B} \rangle$. \mathbf{B}_i is the degree of node i in the collapsed graph, or equivalently the number of distinct neighbors of i in the original graph G . Similarly, Y counts

the total number of edges in the collapsed graph. Define the expectations $\chi = \mathbb{E}[\mathbf{X}]$, $\beta = \mathbb{E}[\mathbf{B}]$, and $\psi = \mathbb{E}[Y]$.

Lemma 3.2 (Second Moment Bounds). *The following inequalities hold: $\text{var}(B_i) \leq u_* \beta_i$, $\text{var}(Y) \leq u_* \psi$, $|\text{cov}(X_{ij}, B_i)| \leq u_* \chi_{ij}$, and $|\text{cov}(X_{ij}, Y)| \leq u_* \chi_{ij}$.*

Proof. We begin by writing

$$\text{var}(B_i) = \text{var}\left(\sum_j X_{ij}\right) = \sum_{j,k} (\mathbb{E}[X_{ij}X_{ik}] - \chi_{ij}\chi_{jk}) = \sum_j (\mathbb{E}[X_{ij}B_i] - \chi_{ij}\beta_i).$$

Next, write $\mathbb{E}[X_{ij}B_i] = \chi_{ij}\mathbb{E}[B_i|X_{ij} = 1]$. The first factor is by definition χ_{ij} . The second factor is bounded above by $\beta_i + u_*$, in which we have taken q to be the identity and $\mathbf{p}(\mathbf{X}) = B_i$. We therefore have

$$\text{var}(B_i) = \sum_j \chi_{ij}(\mathbb{E}[B_i|X_{ij} = 1] - \beta_i) \leq u_* \sum_j \chi_{ij} = u_* \beta_i,$$

which proves the first bound. The second bound is proved via exactly the same calculation, replacing B_i with Y and β_i with ψ . To prove the third bound, we similarly compute

$$\text{cov}(X_{ij}, B_i) = \mathbb{E}[X_{ij}B_i] - \chi_{ij}\beta_i = \chi_{ij}(\mathbb{E}[B_i|X_{ij} = 1] - \beta_i) \leq u_* \chi_{ij},$$

which gives an upper bound on the covariance. Using exactly the same method we obtain a lower bound of $-u_* \chi_{ij}$, proving the result. The proof of the fourth bound runs exactly as the proof of the third, replacing B_i by Y and β_i by ψ . ■

For random variables A and B , define $c(A, B) = \frac{\text{cov}(A, B)}{\mathbb{E}[A]\mathbb{E}[B]}$. We interpret $c(A, B)$ as the relative error associated with factoring expectations, since $\mathbb{E}[AB] = \mathbb{E}[A]\mathbb{E}[B](1 + c(A, B))$. The Cauchy-Schwarz inequality implies that

$$(3.4) \quad |c(A, B)| \leq \frac{\sqrt{\text{var}(A)\text{var}(B)}}{\mathbb{E}[A]\mathbb{E}[B]}.$$

Lemma 3.3. *We have*

$$\delta_{ij}^- = \frac{4\chi_{ij}\psi}{z(m)}(1 + \epsilon^-), \quad \delta_{ij}^+ = \frac{2\beta_i\beta_j}{z(m)}(1 + \epsilon^+),$$

where the error terms satisfy

$$|\epsilon^-| \leq u_* \frac{1 + \beta_i + \beta_j}{2\psi}, \quad |\epsilon^+| \leq u_* \left(\frac{2}{\beta_i \vee \beta_j} + \chi_{ij} \frac{\beta_i + \beta_j + 2}{\beta_i\beta_j} \right).$$

Proof. We require expressions for Δ^- and Δ^+ . These are as in the calculation for the configuration model in [Subsection 3.1](#), except that there now appears an acceptance probability $a((i, j), (k, \ell)) = \frac{1}{W_{ij}W_{k\ell}}$ that appears within each expectation. Performing the algebra and simplifying, we find

$$(3.5) \quad \Delta_{ij}^- = \frac{2}{z(m)} X_{ij} (2Y - (B_i + B_j) + X_{ij})$$

$$(3.6) \quad \Delta_{ij}^+ = \frac{1}{z(m)} 2(B_i - X_{ij})(B_j - X_{ij}) - \langle \mathbf{X}_i, \mathbf{X}_j \rangle.$$

Expanding Equation (3.5) and taking expectations, we have

$$\delta_{ij}^- = \frac{2}{z(m)} (2\mathbb{E}[X_{ij}Y] - \mathbb{E}[X_{ij}(B_i + B_j)] + \chi_{ij}) .$$

By factoring expectations and tracking the error terms, we obtain

$$\delta_{ij}^- = \frac{4\chi_{ij}\psi}{z(m)} \left(1 + c(X_{ij}, Y) - \frac{\beta_i(1 + c(X_{ij}, B_i)) + \beta_j(1 + c(X_{ij}, B_j)) - 1}{2\psi} \right) .$$

In Lemma 3.2 we showed that $|\text{cov}(X_{ij}, B_i)| \leq u_*\chi_{ij}$ and $|\text{cov}(X_{ij}, Y)| \leq u_*\chi_{ij}$. It follows that $|c(X_{ij}, B_i)| \leq u_*\beta_i^{-1}$ and $|c(X_{ij}, Y)| \leq u_*\psi^{-1}$. Applying these bounds and defining ϵ^- as the remaining terms proves the bound on δ_{ij}^- .

Turning to δ_{ij}^+ , we write

$$\begin{aligned} \delta_{ij}^+ &= \frac{1}{z(m)} (2\mathbb{E}[B_i B_j] - 2\mathbb{E}[X_{ij}(B_i + B_j)] - \mathbb{E}[\langle \mathbf{X}_i, \mathbf{X}_j \rangle]) \\ &= \frac{2\beta_i\beta_j}{z(m)} \left(1 + c(B_i, B_j) - \chi_{ij} \frac{\beta_i(1 + c(X_{ij}, B_i)) + \beta_j(1 + c(X_{ij}, B_j))}{\beta_i\beta_j} - \frac{\mathbb{E}[\langle \mathbf{X}_i, \mathbf{X}_j \rangle]}{2\beta_i\beta_j} \right) . \end{aligned}$$

The numerator of the final term is bounded by $\beta_i \wedge \beta_j$. To bound $c(B_i, B_j)$, write

$$\mathbb{E}[B_i B_j] = \sum_k B_i X_{jk} = \sum_k \chi_{jk} \mathbb{E}[B_i | X_{jk} = 1] .$$

Bounding with u_* , we obtain

$$(\beta_i - u_*)b_j \leq \mathbb{E}[B_i B_j] \leq (\beta_i + u_*)\beta_j .$$

Since nothing is special about the choice of i and j , we can symmetrize and simplify, yielding

$$|\text{cov}(B_i, B_j)| = |\mathbb{E}[B_i B_j] - \beta_i\beta_j| \leq u_*(\beta_i \wedge \beta_j) .$$

Dividing through by $\beta_i\beta_j$, we find that $|c(B_i, B_j)| \leq \frac{u_*}{\beta_i \vee \beta_j}$. For the others terms, we recall that $c(X_{ij}, B_i) \leq u_*\chi_{ij}$. Applying these bounds and defining ϵ^+ as the remaining terms proves the result. \blacksquare

We immediately obtain our approximation for χ_{ij} .

Proposition 3.4 (Zeroth Moment of \mathbf{W}). *For all $i \neq j$,*

$$(3.7) \quad \chi_{ij} = f_{ij}(\boldsymbol{\beta})(1 + \epsilon) ,$$

where $|\epsilon| \leq |\epsilon^+| + 2|\epsilon^-| + |\epsilon^+\epsilon^-|$ and where ϵ^+ and ϵ^- are as in Lemma 3.3.

Proof. We set equal the two estimates of Lemma 3.3 and solve for χ_{ij} , obtaining

$$\chi_{ij} = f_{ij}(\boldsymbol{\beta}) \frac{1 + \epsilon^+}{1 + \epsilon^-} .$$

We will choose $\epsilon = (1 + \epsilon^+) / (1 + \epsilon^-) - 1$. To obtain a bound, we note that, since $\epsilon^- \leq \frac{1}{2}$, we have

$$1 - 2\epsilon^- \leq \frac{1}{1 + \epsilon^-} \leq 1 + 2\epsilon^- .$$

From this, we find

$$|\epsilon| = \left| 1 - \frac{1 + \epsilon^+}{1 + \epsilon^-} \right| \leq |\epsilon^+| + 2|\epsilon^-| + |\epsilon^+ \epsilon^-| ,$$

as was to be shown. ■

Proposition 3.4 states that

$$(3.8) \quad \chi_{ij} \approx f_{ij}(\boldsymbol{\beta}) = \frac{\beta_i \beta_j}{2\psi} ,$$

modulo terms that are bounded in terms of the moments of \mathbf{X} and the regularity measure u_* . Speaking somewhat figuratively, we can interpret this result as indicating that \mathbf{X} , the matrix of the projected simple graph, approximately agrees in expectation with the Chung-Lu model (on off-diagonal entries) with parameter vector $\boldsymbol{\beta}$. It would be incorrect to interpret this equation as stating that \mathbf{X} is distributed according to any model that deterministically preserves a collapsed degree sequence. First, $\boldsymbol{\beta}$ does not in general possess integer entries. Second the collapsed degrees B_i are still stochastic, and preserved only approximately in expectation.

3.3. First Moments of \mathbf{W} . In the case of the configuration model, approximately solving the $p = 1$ stationarity condition yielded an approximation for $\boldsymbol{\omega}$ in terms of the known vector \mathbf{d} . However, in the uniform model we derived an approximation only for $\boldsymbol{\chi}$ in terms of the unknown vector $\boldsymbol{\beta}$. Computing another equilibrium condition will allow us to both estimate $\boldsymbol{\omega}$ from $\boldsymbol{\chi}$ and learn $\boldsymbol{\beta}$ from \mathbf{d} . Take $p = 2$ in [Equation \(3.1\)](#), obtaining

$$(3.9) \quad 2\mathbb{E}[W_{ij}\Delta_{ij}] + \mathbb{E}[\Delta_{ij}^2] = 0 .$$

The second term can be calculated from previous results, since $\mathbb{E}[\Delta_{ij}^2] = \delta_{ij}^+ + \delta_{ij}^-$. We therefore focus on the first.

Lemma 3.5. *We have*

$$\mathbb{E}[W_{ij}\Delta_{ij}] = \frac{2\omega_{ij}b_i b_j(1 + \epsilon_1) - 4\omega_{ij}\psi(1 + \epsilon_3) - \epsilon_2}{z(m)} ,$$

where:

$$\begin{aligned} |\epsilon_1| &\leq \frac{u_*}{\beta_i \vee \beta_j} + \frac{\sigma_{ij} \sqrt{2u_*(\beta_i + \beta_j + 2u_*)(\beta_i \beta_j + u_*(\beta_i \wedge \beta_j))}}{\omega_{ij} \beta_i \beta_j} , \\ |\epsilon_2| &\leq \omega_{ij}(\beta_i \wedge \beta_j) \left(1 + \frac{u_* \sigma_{ij}}{\omega_{ij} \sqrt{\beta_i \vee \beta_j}} \right) , \\ |\epsilon_3| &\leq \frac{u_* \sigma_{ij}}{\omega_{ij} \sqrt{\psi}} . \end{aligned}$$

Proof. We can write out

$$\mathbb{E}[W_{ij}\Delta_{ij}] = \mathbb{E}[W_{ij}(\Delta_{ij}^+ - \Delta_{ij}^-)] = \frac{1}{z(m)}\mathbb{E}[(2W_{ij}B_iB_j - W_{ij}\langle X_i, X_j \rangle - 4W_{ij}Y)].$$

We will bound each of these terms using simple second moment methods. Starting with the last,

$$\mathbb{E}[W_{ij}Y] = \omega_{ij}\psi(1 + c(W_{ij}, Y)).$$

Applying Cauchy-Schwarz and [Lemma 3.2](#), the error term, which we call ϵ_3 , can be bounded by $|c(W_{ij}, Y)| \leq u_*\sigma_{ij}(\omega_{ij}\sqrt{\psi})^{-1}$.

The middle term is comparatively small in magnitude. Call it ϵ_2 , and write

$$\epsilon_2 = \mathbb{E}[W_{ij}\langle \mathbf{X}_i, \mathbf{X}_j \rangle] \leq \mathbb{E}[W_{ij}B_i] = \omega_{ij}\beta_i(1 + c(W_{ij}, B_i)).$$

Applying Cauchy-Schwarz and [Lemma 3.2](#) again, $|c(W_{ij}, B_i)| \leq u_*\sigma_{ij}(\omega_{ij}\sqrt{\beta_i})^{-1}$. Since we could just as easily have written $\epsilon_2 \leq \mathbb{E}[W_{ij}B_j]$, we can tighten the bound slightly, obtaining

$$|\epsilon_2| \leq \omega_{ij}(\beta_i \wedge \beta_j) \left(1 + \frac{u_*\sigma_{ij}}{\omega_{ij}\sqrt{\beta_i \vee \beta_j}} \right).$$

Finally, we consider the first term, which is somewhat more challenging to bound. Write

$$(3.10) \quad \mathbb{E}[W_{ij}B_iB_j] = \omega_{ij}\beta_i\beta_j \left(1 + c(B_i, B_j) + \frac{\text{cov}(W_{ij}, B_iB_j)}{\omega_{ij}\beta_i\beta_j} \right).$$

We have already seen that $|c(B_i, B_j)| \leq \frac{u_*}{\beta_i \vee \beta_j}$ in the proof of [Lemma 3.3](#). To bound the covariance, we apply Cauchy-Schwarz. For this we need control over the quantity $\text{var}(B_iB_j)$. We can write

$$\begin{aligned} \mathbb{E}[B_i^2B_j^2] &= \sum_{k,\ell} \mathbb{E}[B_iB_jX_{ik}X_{j\ell}] \\ &= \sum_{k,\ell} \mathbb{E}[X_{ik}X_{j\ell}]\mathbb{E}[B_iB_j|X_{ik}X_{j\ell} = 1] \\ &\leq \sum_{k,\ell} \mathbb{E}[X_{ik}X_{j\ell}]\mathbb{E}[(B_i + 2u_*)(B_j + 2u_*)] \\ &= \mathbb{E}[B_iB_j]\mathbb{E}[(B_i + 2u_*)(B_j + 2u_*)] \\ &= \mathbb{E}[B_iB_j]^2 + 2u_*(\beta_i + \beta_j + 2u_*)\mathbb{E}[B_iB_j]. \end{aligned}$$

From the proof of [Lemma 3.3](#), we have that $\mathbb{E}[B_iB_j] \leq \beta_i\beta_j + u_*\beta_i \wedge \beta_j$. Applying this result, we find that $\text{var}(B_iB_j) \leq 2u_*(\beta_i + \beta_j + 2u_*)(\beta_i\beta_j + u_*(\beta_i \wedge \beta_j))$. Defining ϵ_1 as in the statement of the lemma and applying Cauchy-Schwarz, we have obtained

$$|\epsilon_1| \leq \frac{u_*}{\beta_i \vee \beta_j} + \frac{\sigma_{ij}\sqrt{2u_*(\beta_i + \beta_j + 2u_*)(\beta_i\beta_j + u_*(\beta_i \wedge \beta_j))}}{\omega_{ij}\beta_i\beta_j},$$

which completes the proof. ■

Proposition 3.6 (First Moments of \mathbf{W}). *We have*

$$(3.11) \quad \omega_{ij} = \frac{\chi_{ij}}{1 - \chi_{ij}}(1 + \mathcal{E}),$$

where \mathcal{E} is a polynomial in the error terms ϵ appearing in Proposition 3.4 and Lemmas 3.3 and 3.5.

Proof. Inserting the above results and Lemma 3.3 into the $p = 2$ stationarity condition yields, after running the algebra,

$$\begin{aligned} \omega_{ij} &= \frac{1}{2z(m)} \frac{\delta_{ij}^+ + \delta_{ij}^- + \epsilon_2}{4\psi(1 + \epsilon_3) - 2b_i b_j(1 + \epsilon_1)} \\ &= \frac{1}{2} \frac{\chi_{ij}(1 + \epsilon)^{-1}(1 + \epsilon^+) + \chi_{ij}(1 + \epsilon^-) + \epsilon_2/z(m)}{(1 + \epsilon_3) - \chi_{ij}(1 + \epsilon)^{-1}(1 + \epsilon_1)}. \end{aligned}$$

To prove the proposition, we simply collect the error terms within \mathcal{E} . ■

Recalling that $\chi_{ij} = \eta_{\mathbf{d}}(W_{ij} \geq 1)$, Equation (3.11) states that ω_{ij} is approximately equal to the odds that there is at least one edge present between nodes i and j . As we will see, this approximation gives us a method to compute the vector β in terms of the vector \mathbf{d} , thereby obtaining an approximation for the moments of \mathbf{W} .

3.4. Second Moments. Before proceeding, we briefly comment on the $p = 3$ stationarity condition. From this case on, it becomes quite tedious to control the error terms associated with factoring expectations. Omitting them, we obtain the approximation

$$\mathbb{E}[W_{ij}^2] \approx \omega_{ij} \left(\omega_{ij} + \frac{1}{1 - \chi_{ij}} \right).$$

It follows that

$$(3.12) \quad \sigma_{ij}^2 \triangleq \text{var}(W_{ij}) \approx \frac{\chi_{ij}}{(1 - \chi_{ij})^2} \approx \omega_{ij}(\omega_{ij} + 1).$$

Note that, under this approximation, $\sigma_{ij}^2 > \omega_{ij}$ whenever $\chi_{ij} > 0$. It is common to model the entries of the adjacency matrix as Poisson random variables, for which the mean and variance are equal. Equation (3.12) suggests that this approach will be approximately correct for the uniform model when $\omega_{ij} \ll 1$, but systematically underestimate the variance for larger values.

4. Estimation of β . We now possess approximate formulae for the zeroth, first, and second moments of W in terms of the vector β . In practice, we do not observe β and must therefore estimate it from \mathbf{d} . Inserting Equation (3.8) into Equation (3.11) yields the approximation

$$\omega_{ij} \approx \frac{\beta_i \beta_j}{2\psi - \beta_i \beta_j}$$

for any $i \neq j$. Imposing the degree constraint $\sum_j \omega_{ij} = d_i$, we obtain

$$(4.1) \quad d_i \approx h_i(\boldsymbol{\beta}) \triangleq \sum_j \frac{\beta_i \beta_j}{2\psi - \beta_i \beta_j}.$$

In this expression, the function $\mathbf{h} : \mathbb{R}^n \rightarrow \mathbb{R}^n$ approximately maps the collapsed degree sequence $\boldsymbol{\beta}$ to the uncollapsed degree sequence \mathbf{d} (ignoring error terms). Operationally, we treat [Equation \(4.1\)](#) as exact and define the estimator $\hat{\boldsymbol{\beta}}$ of $\boldsymbol{\beta}$ as its solution. We then construct $\hat{\boldsymbol{\omega}}^1 = \mathbf{f}(\hat{\boldsymbol{\beta}})$ as our estimator for $\boldsymbol{\omega}$.

In order to develop a solution method for [Equation \(4.1\)](#), it is informative to compute the partial derivatives of h with respect to the components of $\boldsymbol{\beta}$. We find

$$(4.2) \quad \frac{\partial h_i(\boldsymbol{\beta})}{\partial \beta_k} = \begin{cases} \sum_{j \neq i} \beta_j \frac{2\psi - \beta_i}{(2\psi - \beta_i \beta_j)^2} & i = k \\ \frac{2\psi \beta_i - 1}{(2\psi - \beta_i \beta_k)^2} - \sum_{j \neq i} \frac{\beta_i \beta_j}{(2\psi - \beta_i \beta_j)^2} & i \neq k. \end{cases}$$

The diagonal component is usually much larger than either term in the off-diagonal components. This observation suggests that [Equation \(4.1\)](#) may be efficiently solved by decoupling coordinates. We first initialize $\hat{\boldsymbol{\beta}}^{(0)}$. For each i , we solve $h_i(\hat{\boldsymbol{\beta}}^{(0)}) = d_i$ for the i th coordinate $\hat{\beta}_i^{(0)}$, holding the other coordinates of $\hat{\boldsymbol{\beta}}^{(0)}$ fixed. The following technical lemma assures us that this is possible.

Lemma 4.1. *Let h_i be the i th component of h . Fix all components of $\boldsymbol{\beta}$ but β_i . Let $I = (0, \frac{2\psi - \beta_i}{\max_{j \neq i} \beta_j})$. Then,*

1. *The function h_i , regarded as a function of β_i , is continuously differentiable and monotonically increasing on I .*
2. *If $\beta_j > 0$ for all $j \neq i$, then if $\beta_i = 0$, then $h_i(\boldsymbol{\beta}) = 0$.*
3. *If $\beta_j > 0$ for all $j \neq i$, $\sup_{\beta_i \in I} h_i(\boldsymbol{\beta}) = \infty$.*

Proof. Continuous differentiability follows from inspecting [Equation \(4.2\)](#) and noting that all components are continuous functions on I . Monotonicity follows from the fact that $\partial h_i(\boldsymbol{\beta}) / \partial \beta_i > 0$. Next, if $\beta_i = 0$, $h_i(\boldsymbol{\beta}) = 0$ unless $y = 0$; the condition on $\boldsymbol{\beta}$ prevents this. Finally, approaching the upper limit of I from below shrinks the denominator in [Equation \(4.1\)](#), causing the value of $h_i(\boldsymbol{\beta})$ to grow without bound. \blacksquare

[Lemma 4.1](#) ensures that, under mild conditions, a unique solution to the equation $h_i(\boldsymbol{\beta}) = d_i$ in the coordinate β_i exists on the interval I . So long as the initial value $\hat{\beta}_i^{(0)}$ lies within this interval, standard algorithms such as bisection search or Newton-type methods can be used to identify the solution.

Because the variables $\hat{\boldsymbol{\beta}}$ are truly coupled through h , a single sweep through the components of $\hat{\boldsymbol{\beta}}$ will not guarantee that the equation $\mathbf{h}(\hat{\boldsymbol{\beta}}) = \mathbf{d}$ holds even approximately. We therefore repeat the sweep iteratively until the change in $\hat{\boldsymbol{\beta}}$ decreases below some specified

threshold. Formally,

Algorithm 2: Computation of β

Input: degree sequence $d \in \mathbb{Z}_+^n$, initial guess $\hat{\beta}^{(0)} \in \mathbb{R}_+^n$, tolerance ϵ

1 **Initialization:** $t \leftarrow 0$, $\gamma \leftarrow \infty$

2 **while** $\gamma > \epsilon$ **do**

3 **for** $i = 1, \dots, n$ **do**

4 $\hat{\beta}_i^{(t)} \leftarrow \text{Solve}_i\{f_i(\hat{\beta}^{(t-1)}) - d_i = 0\}$

5 $\gamma \leftarrow \left\| \hat{\beta}^{(t)} - \hat{\beta}^{(t-1)} \right\|^2$

6 $t \leftarrow t + 1$

Output: $\hat{\beta}^{(t)}$

The subroutine Solve_i solves the given equation for the i th coordinate while keeping all others constant. We implemented this subroutine using Newton’s method, with the required derivative provided by Equation (4.2), but many alternatives could be used.

Because Algorithm 2 discards the error terms that appear in Equation (3.11), an exact statistical guarantee relating the estimator $\hat{\beta}$ to β does not appear to be possible. There is also a minor convergence issue. If in a given inner iteration, $\hat{\beta}_i^{(t)}$ is initialized outside the interval I , then the Solve_i subroutine is not guaranteed to converge to the expected value, potentially leading the entire algorithm to fail. In experiments, we did observe that this behavior can occur. However, pre-sorting the degree sequence \mathbf{d} (so that small-degree nodes are touched earlier in the sweep) was sufficient to ensure convergence under reasonable initial guesses. For example, the choice $\hat{\beta}^{(0)} = \mathbf{e}$ (as implemented in the provided code) appears to always converge correctly. Adversarial choices of $\hat{\beta}^{(0)}$, such as initializing $\hat{\beta}^{(0)} = s\mathbf{e}_1$ for large s , were necessary to prevent rapid convergence.

5. Experiments with Dense Contact Networks. Our main study data set is `contact-high-school` a contact network among students in a French secondary school [22, 4]. During data collection, each student wore a proximity sensor. An interaction between two students was logged by their respective sensors when the students were face-to-face and within approximately 1.5m of each other. Edges are time-stamped, although we do not use any temporal information in this study. The original data set contains $n = 327$ nodes and $m = 189,928$ distinct interactions.

5.1. Evaluation. We first test the accuracy of the estimator $\hat{\omega}^1$, using $\hat{\Omega}^{\text{mc}}$ as a reliable estimate of the true mean ω . Because of the scaling issues associated with estimating $\hat{\Omega}^{\text{mc}}$ on $m \approx 2 \times 10^5$ edges, we constructed a data subset based on a temporal threshold τ , chosen to incorporate approximately the last 5% of the original interaction volume. The resulting subnetwork has 268 nodes and 10,026 edges. We were able to estimate $\hat{\Omega}^{\text{mc}}$ using $k = 10,000$ samples in roughly three days on personal computing equipment.

In Figure 1(a)-(b), we show the distributions of degrees and entries of \mathbf{w} for this subnetwork. Figure 1(a) depicts the heterogenous degree distribution, with standard deviation larger than the average degree. While most nodes have small degrees, there are twelve whose degree exceeds n . Figure 1(b) shows the clumping of edges between pairs of nodes. On

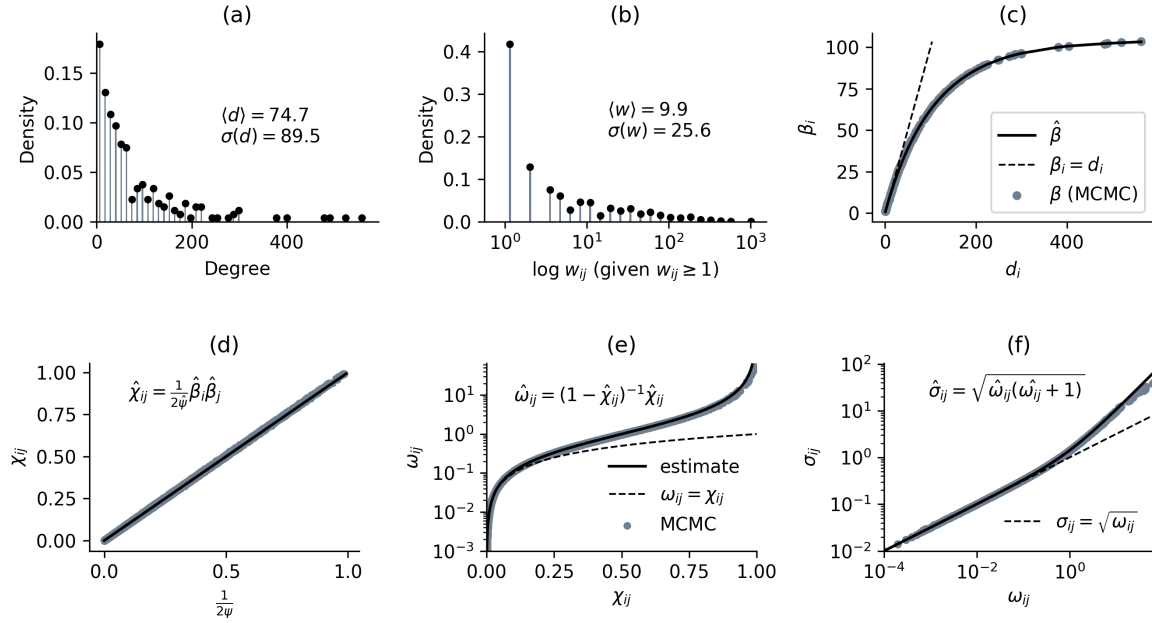


Figure 1: (a): Degree distribution of the **contact-high-school** subnetwork. The mean degree $\langle d \rangle$ and standard deviation of the degree $\sigma(d)$ are shown. (b): Distribution of the entries of \mathbf{w} . Note the logarithmic horizontal axis. (c): Collapsed degree sequence $\hat{\beta}$ learned from \mathbf{d} via [Algorithm 2](#). Dashes give the line of equality. (d): Approximation of χ via [Equation \(3.8\)](#). (e): Approximation of ω via [Equation \(3.11\)](#). Note the logarithmic vertical axis. Dashes give the line of equality. (f): Approximation of $\sigma_{ij} = \sigma(W_{ij})$ via [Equation \(3.12\)](#). Note the log-log axis. In (d)-(f), simulated moments are obtained from $k = 10,000$ samples from [Algorithm 1](#) with sample interval $9,237 \approx \frac{m \log m}{10}$ steps.

average, two students who interact at all interact nearly ten times, but there is substantial deviation around this average. Almost half of all pairs interact just once. In contrast, a small number of pairs interact over 100 times, and one over 1,000.

In [Figure 1\(c\)-\(f\)](#), we show the construction of estimators for the moments of W under the uniform random graph model with the observed degree sequence \mathbf{d} . In [Figure 1\(c\)](#), the solid line shows the estimate $\hat{\beta}$ output by [Algorithm 2](#), plotted against the degree sequence. Points give the MCMC estimate for β . The agreement is almost exact. In [Figure 1\(d\)](#), we estimate $\hat{\chi}_{ij} \approx f_{ij}(\hat{\beta}) = \frac{\hat{\beta}_i \hat{\beta}_j}{2\hat{\psi}}$, again finding the agreement to be near exact. In (e), we estimate $\hat{\omega}_{ij} \approx (1 - \hat{\chi}_{ij})^{-1} \hat{\chi}_{ij}$. The agreement with data is again excellent, although there is a small amount of visible overestimation of ω_{ij} when χ_{ij} is large. Finally, (f) uses [Equation \(3.12\)](#) to compute an estimator $\hat{\sigma}_{ij} = \sqrt{\hat{\omega}_{ij}(\hat{\omega}_{ij} + 1)}$ of σ_{ij} the standard deviation of W_{ij} . The agreement is strong through roughly $\omega_{ij} \approx 10$, and begins to overestimate σ_{ij} for larger values.

[Figure 1\(c\)](#) and (e) also help to highlight the relationship of $\hat{\omega}^1$ and $\hat{\omega}^0$. The dashed lines in these figures represent two linear approximations that can be made to yield the latter

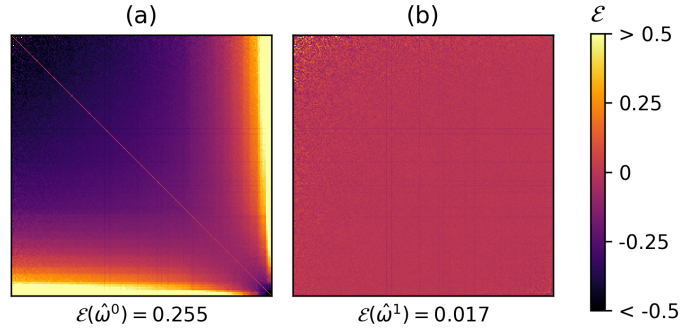


Figure 2: Shading gives the relative error for approximating ω under the uniform model for the `contact-high-school` subnetwork. (a): Using the CL estimator $\hat{\omega}^0$. (b): Using $\hat{\omega}^1$. Node degrees in each matrix increase left to right and top to bottom. The “ground truth” is provided by $\hat{\Omega}^{\text{mc}}$, computed as in [Figure 1](#).

from the former. First, we approximate $\beta = \mathbf{d}$ (dashed line, [Figure 1\(c\)](#)). This approximation holds good when d_i is small, since then the number of parallel edges incident to node i should be small – i.e. $W_{ij} \approx X_{ij}$. Then, we approximate $\omega = \chi$ (dashed line, [Figure 1\(e\)](#)). This approximation should hold for small entries of ω , since in this case χ_{ij} is small and $(1 - \chi_{ij})^{-1} \approx 1$. As the plots indicate, these approximations are indeed accurate when d_i and ω_{ij} are small. These conditions correspond roughly to the “large, sparse” heuristics used frequently in the literature. We can therefore view $\hat{\omega}^0$ as a first-order approximation to $\hat{\omega}^1$ near the large, sparse regime. Conversely, we can view $\hat{\omega}^1$ as a nonlinear correction to $\hat{\omega}^0$ as we depart from that regime.

[Figure 2](#) compares the overall performance of the estimators $\hat{\omega}^0$ and $\hat{\omega}^1$. We compute the entrywise relative error $\mathcal{E}_{ij}(\hat{\omega}) = (\hat{\Omega}_{ij}^{\text{mc}})^{-1}(\hat{\omega}_{ij} - \hat{\Omega}_{ij}^{\text{mc}})$ when approximating $\hat{\Omega}^{\text{mc}} \approx \omega$ with both methods. Cells are shaded according to the magnitude and sign of the error. Similar to the synthetic data set above, the CL estimator in (a) displays systematic bias, underestimating the density of edges between nodes of similar degrees and overestimating the density of edges between nodes with highly disparate degrees. The mean absolute relative error of the Chung-Lu estimate is $\mathcal{E}(\hat{\omega}^0) = \binom{n}{2}^{-1} \sum_{ij} |\mathcal{E}_{ij}(\hat{\omega}^0)| \approx .255$, indicating that a typical entry of $\hat{\omega}^0$ is off by over 25%. In contrast, $\hat{\omega}^1$ evaluated in (b) has almost no visible bias and a mean absolute relative error $\mathcal{E}(\hat{\omega}^1) < 2\%$. This is a full order of magnitude improvement when compared to $\hat{\omega}^0$.

5.2. Modularity Maximization in a Dense Contact Network. Let $\ell : N \rightarrow \mathcal{L}$ be a function that assigns to node i a label $\ell_i \in \mathcal{L}$. The *modularity* of the partition ℓ with respect to matrix \mathbf{w} and null model ρ is given by

$$(5.1) \quad Q(\ell; \rho) = \frac{1}{2m} \sum_{ij} [w_{ij} - \mathbb{E}_\rho[W_{ij}]] \delta(\ell_i, \ell_j),$$

where $\delta(\ell_i, \ell_j) = \mathbb{1}(\ell_i = \ell_j)$. The normalization by $2m$ ensures that $-1 \leq Q(\ell; \rho) \leq 1$. Intuitively, $Q(\ell; \rho)$ is high when nodes that are more densely connected than expected by chance (under the specified null) are grouped together. Maximizing this quantity with respect to ℓ may therefore be reasonably expected to identify modular (“community”) structure in the network [26, 28]. Exact modularity maximization is NP-hard [15] and subject to theoretical limitations in networks with modules of heterogeneous sizes [17]. Despite this, it remains one of the most popular methods for practical community detection at scale [6].

In most implementations, ρ is not explicitly specified – rather, the expectation $\mathbb{E}_\rho[W_{ij}]$ is “hard-coded” as equal to $\hat{\omega}_{ij}^0$. From a statistical perspective, this reflects an implicit choice of ρ as the Chung-Lu model [12], which preserves expected degrees and indeed possesses the given first moment.³ Modifications are possible; the best known is perhaps the resolution adjustment that replaces $\hat{\omega}^0$ with $\gamma\hat{\omega}^0$ for some $\gamma > 0$ [30]. Other adjustments may incorporate spatial structure [16] or adjust for the inclusion of self-loops in the null space [8]. When we wish to perform modularity maximization against a null that deterministically preserves degree sequences, $\hat{\omega}^0$ is at best an approximation. We expect this approximation to perform adequately for the configuration model (cf. [Theorem 3.1](#)), and very poorly for the uniform model (previous subsection). In the latter case, estimator $\hat{\omega}^1$ can be used instead, including on data sets for which the computation of $\hat{\Omega}^{\text{mc}}$ is intractable.

In this experiment, we illustrate the importance of the choice between Chung-Lu and uniform null expectations for modularity maximization on a dense multigraph. Computation of $\hat{\Omega}^{\text{mc}}$ is not feasible for graph this dense, and we therefore use $\hat{\omega}^1$ as an estimate, supposing its performance to be similar on the full network as on the subnetwork in the previous section. This setting highlights the utility of $\hat{\omega}^1$, since otherwise we would have no practical way to compute the uniform expectation.

We employ the multiway spectral partitioning (MSP) algorithm of [37], which generalizes the spectral graph bipartitioning algorithm of [26]. While greedy methods often enjoy superior performance [6], spectral methods have the advantage of depending strongly on the structure of the observed graph and the null model employed, and are relatively insensitive to choices made during the runtime of the algorithm. Spectral methods are therefore ideal for highlighting differences in the modularity landscapes induced by alternative null models. The method requires the analyst to specify a null model and a desired number of communities k . The core of the approach is to use a low-rank approximation of the *modularity matrix*, $\mathbf{M} = \mathbf{w} - \mathbb{E}_\rho[\mathbf{W}]$. This approximation induces a map from the vertices of G to a low-dimensional vector space. Vectors in this space are clustered according to their relative angles using a procedure reminiscent of k -means to produce the community assignment. Because the clustering algorithm involves a stochastic starting condition, it is useful to run the algorithm multiple times and choose the highest modularity partition from among the repetitions. We refer the reader to [37] for details, and to the code accompanying this paper for an implementation of MSP.

We ran this algorithm using both the CL modularity matrix $\mathbf{M}^0 = \mathbf{w} - \hat{\omega}^0$ and the approximate uniform modularity matrix $\mathbf{M}^1 = \mathbf{w} - \hat{\omega}^1$. We refer to these two algorithmic variants as MSP^0 and MSP^1 , respectively. Since $\hat{\omega}^0$ and $\hat{\omega}^1$ produce very different null matrices, the

³We note that alternative justifications of the use of $\hat{\omega}^0$ exist, including connections to the stability of Markov chains [14] and to stochastic block models [27].

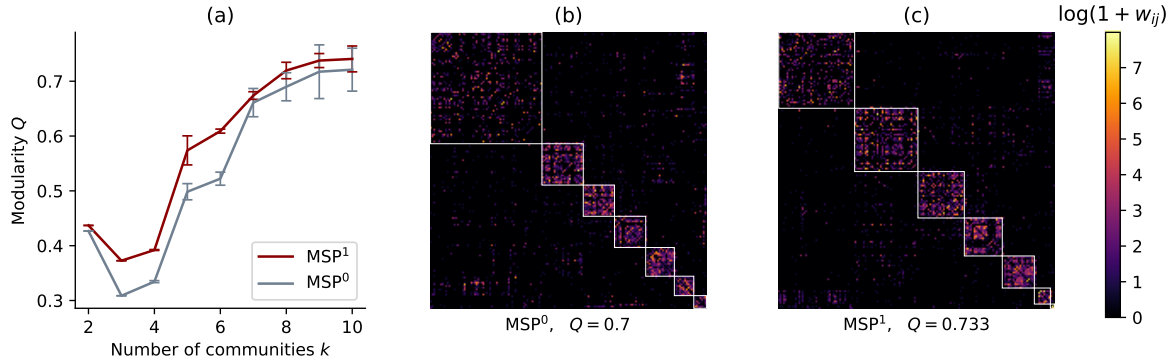


Figure 3: (a): Performance of MSP using the CL modularity matrix \mathbf{M}^0 and the approximate uniform modularity matrix \mathbf{M}^1 , over 100 batches of 50 repetitions each. Solid lines give the average modularity, and error bars give two standard deviations from the mean. (b): Example partition using \mathbf{M}^0 . (c): Example partition using \mathbf{M}^1 . To generate (b) and (c), the best partition of 500 runs was chosen for each algorithm variant. Each run was initialized with $k = 8$; in the best partition, however, only 7 labels are actually used. Colors are shown on a log scale.

modularity matrices \mathbf{M}^0 and \mathbf{M}^1 are themselves very different – the mean absolute relative error of using the latter to estimate the former is approximately 32%. We would therefore expect MSP^0 and MSP^1 to behave very differently in this task. We allowed the number of communities k to vary between 2 and 10. For each value of k , we ran MSP^0 and MSP^1 in 100 batches of 50 repetitions. From each batch of 50, the highest-modularity partition was chosen, resulting in 100 partitions per value of k . Figure 3(a) shows that MSP^1 tends to find higher modularity partitions than MSP^0 on this data set. The difference is especially large when k is small, but a substantial difference between the means is noticeable even for larger values. While partitions under \mathbf{M}^0 exist that are comparable to those under \mathbf{M}^1 , it appears to be more difficult for MSP^0 to find them. Panels (b) and (c) shed some light on the differing behavior of the two algorithms. Partitions under MSP^0 tends to display a larger, less cohesive community ((b), top left) alongside smaller, more tightly interconnected ones. Partitions under MSP^1 (c) tend to display communities that are slightly more uniform in size.

It is reasonable to object that modularity values under MSP^1 and MSP^0 should not be compared, since these objectives are defined with respect to differing null matrices. This objection is not borne out numerically, however – “cross-evaluating” the partitions on the opposite matrices changes the modularities only minimally. Evaluating the MSP^0 partition in Figure 3(b) on the modularity matrix \mathbf{M}^1 gives $Q = 0.699$, while evaluating the MSP^1 partition on \mathbf{M}^0 yields $Q = 0.731$. On this data set, MSP^1 searches the energy landscape of MSP^0 more efficiently than does MSP^0 itself.

It should be noted that this behavior is data-set dependent. The opposite case occurs in the `contact-primary-school` network [32, 4], which used similar sensors to construct an interaction network among students in a French primary school. On this data, MSP^0

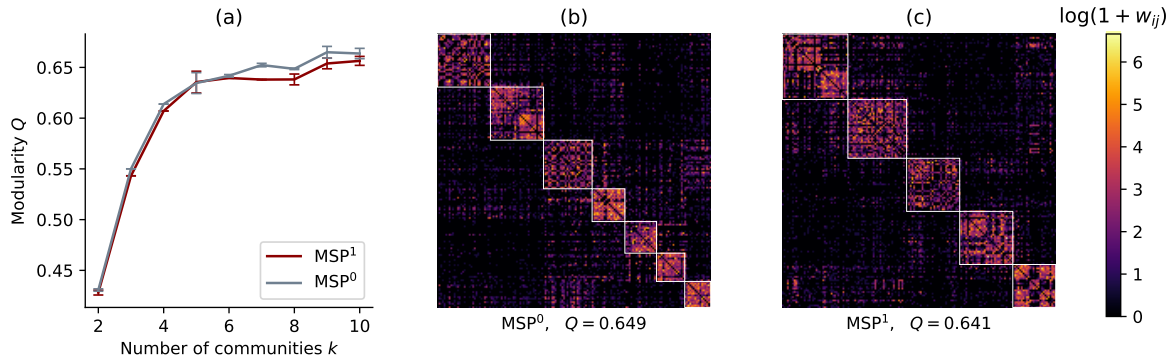


Figure 4: This figure is in all methodological details identical to [Figure 3](#), using the study data set `contact-primary-school` [33, 4]. In (b)-(c), both algorithms were initialized with $k = 8$.

and MSP^1 perform similarly for $k \leq 6$ communities ([Figure 4](#)), with the former consistently outperforming the latter for $k \geq 7$. The illustrative partitions in panels (b) and (c) suggest MSP^1 tends to prefer partitions with fewer communities. Whereas MSP^0 chooses a partition with 7 communities, MSP^1 chooses one with just 5 (both having been initialized at $k = 8$). These illustrations emphasize that MSP^1 and MSP^0 explore different modularity landscapes; that the relative advantages of each algorithm depend on the data; and that the landscape for MSP^1 can be tractably computed under the methodology we have introduced here.

6. Discussion. Much of network theory is explicitly designed for studying large, sparse networks. However, many data sets of interest are sufficiently dense to diverge significantly from the predictions of large, sparse theory. We have highlighted this phenomenon in the context of dense multigraphs, with a focus on estimating the expected adjacency matrix ω of a random multigraph with specified degree sequence. We have shown that, rather than falling back to computationally expensive MCMC, we can construct an accurate estimator $\hat{\omega}^1$ using an indirect, dynamical approach. Use of this estimator can in turn have significant impact on the results of downstream data analyses.

There are several directions for future work on the moments of uniform random graphs with fixed degree sequences. As previously noted, the error bounds on $\hat{\chi}$ and $\hat{\omega}^1$ derived in [Section 3](#) appear quite loose when compared against the empirical results in [Figure 1](#). The derivation of tighter error bounds would be helpful for researchers seeking practical accuracy guarantees. Progress on this front appears to be hindered by the complex combinatorial structure of the space $\mathcal{G}_{\mathbf{d}}$; however, carefully-chosen assumptions or approximations may allow headway. Another interesting theoretical question concerns the relation of β and \mathbf{d} . We have estimated the former from the latter numerically, but there may well exist a closed-form expression that relates the two. Such an expression would eliminate the need for [Algorithm 2](#), thereby making $\hat{\omega}^1$ just as easy to compute as $\hat{\omega}^0$. An additional avenue of exploration concerns the impact of the choice between $\hat{\omega}^1$ and $\hat{\omega}^0$ on downstream analyses. We saw in [Section 5](#) that the choice of null expectation can substantially change the performance of MSP,

and that the direction of this effect depends on the data set. A better understanding of the properties of the data or algorithm that make certain estimators highlight better solutions would be most welcome.

We focused our attention on the derivation of an estimator for ω . It may also be possible to derive expressions for higher moments using the same methodology. Such moments would approximate expected densities of various motifs under the uniform model. Examples of interest may include wedge densities $\mathbb{E}[W_{ij}W_{jk}]$ and triangle densities $\mathbb{E}[W_{ij}W_{jk}W_{ik}]$. Parsing the stationarity conditions for these more complicated moments may be correspondingly more difficult. An alternative would be to construct mean-field estimates by computing the relevant statistics on $\hat{\omega}^1$ itself. An evaluation of the accuracy of this approach would potentially replace the need for computationally intensive MCMC sampling to estimate these quantities.

Software. We used the implementation of vertex-labeled MCMC in [10] to conduct simulation experiments. All additional code used in this study may be freely accessed at https://github.com/PhilChodrow/multigraph_moments.

REFERENCES

- [1] G. AMANATIDIS, B. GREEN, AND M. MIHAIL, *Graphic realizations of joint-degree matrices*, arXiv preprint arXiv:1509.07076, (2015), pp. 1–18.
- [2] O. ANGEL, R. VAN DER HOFSTAD, AND C. HOLMGREN, *Limit laws for self-loops and multiple edges in the configuration model*, arXiv:1603.07172, (2016), pp. 1–19.
- [3] Y. ARTZY-RANDRUP AND L. STONE, *Generating uniformly distributed random networks*, Phys. Rev. E, 72 (2005), p. 056708, <https://doi.org/10.1103/PhysRevE.72.056708>.
- [4] A. R. BENSON, R. ABEBE, M. T. SCHAUB, A. JADBABAIE, AND J. KLEINBERG, *Simplicial closure and higher-order link prediction*, Proceedings of the National Academy of Sciences, 115 (2018), pp. 11221–11230.
- [5] J. BLITZSTEIN AND P. DIACONIS, *A sequential importance sampling algorithm for generating random graphs with prescribed degrees*, Internet mathematics, 6 (2011), pp. 489–522.
- [6] V. D. BLONDEL, J.-L. GUILLAUME, R. LAMBIOTTE, AND E. LEFEBVRE, *Fast unfolding of communities in large networks*, Journal Of Statistical Mechanics-Theory And Experiment, 10 (2008), pp. 1–12.
- [7] B. BOLLOBÁS, *A probabilistic proof of an asymptotic formula for the number of labelled regular graphs*, European Journal of Combinatorics, 1 (1980), pp. 311–316.
- [8] S. CAFIERI, P. HANSEN, AND L. LIBERTI, *Loops and multiple edges in modularity maximization of networks*, Physical Review E, 81 (2010), p. 046102.
- [9] C. J. CARSTENS, *Proof of uniform sampling of binary matrices with fixed row sums and column sums for the fast curveball algorithm*, Physical Review E, 91 (2015), p. 042812.
- [10] P. S. CHODROW, *Configuration models of random hypergraphs*, arXiv: 1902.09302v2, (2019), pp. 1–20, <https://arxiv.org/abs/1902.09302v1>.
- [11] F. CHUNG AND L. LU, *Connected components in random graphs with given expected degree sequences*, Annals of Combinatorics, 6 (2002), pp. 125–145.
- [12] F. CHUNG AND L. LU, *The average distances in random graphs with given expected degrees*, Proceedings of the National Academy of Sciences, 99 (2002), pp. 15879–15882.
- [13] C. I. DEL GENIO, H. KIM, Z. TOROCZKAI, AND K. E. BASSLER, *Efficient and exact sampling of simple graphs with given arbitrary degree sequence*, PloS one, 5 (2010), p. e10012.
- [14] J. C. DELVENNE, S. N. YALIRAKI, AND M. BARAHONA, *Stability of graph communities across time scales*, Proceedings of the National Academy of Sciences, (2010), <https://doi.org/10.1073/pnas.0903215107>.
- [15] T. N. DINH, X. LI, AND M. T. THAI, *Network clustering via maximizing modularity: Approximation algorithms and theoretical limits*, Proceedings - IEEE International Conference on Data Mining, ICDM, 2016-January (2016), pp. 101–110, <https://doi.org/10.1109/ICDM.2015.139>.

- [16] P. EXPERT, T. S. EVANS, V. D. BLONDEL, AND R. LAMBIOTTE, *Uncovering space-independent communities in spatial networks*, Proceedings of the National Academy of Sciences, 108 (2011), pp. 7663–7668.
- [17] S. FORTUNATO AND M. BARTHÉLEMY, *Resolution limit in community detection*, Proceedings of the National Academy of Sciences, 104 (2006), pp. 36–41.
- [18] B. K. FOSDICK, D. B. LARREMORE, J. NISHIMURA, AND J. UGANDER, *Configuring random graph models with fixed degree sequences*, SIAM Review, 60 (2018), pp. 315–355.
- [19] C. GREENHILL, *A polynomial bound on the mixing time of a markov chain for sampling regular directed graphs*, The Electronic Journal of Combinatorics, 18 (2011), p. 234.
- [20] C. GREENHILL, *The switch markov chain for sampling irregular graphs*, in Proceedings of the Twenty-Sixth Annual ACM-SIAM Symposium on Discrete Algorithms, SIAM, 2014, pp. 1564–1572.
- [21] M. JERRUM AND A. SINCLAIR, *Fast uniform generation of regular graphs*, Theoretical Computer Science, 73 (1990), pp. 91–100.
- [22] R. MASTRANDREA, J. FOURNET, AND A. BARRAT, *Contact patterns in a high school: A comparison between data collected using wearable sensors, contact diaries and friendship surveys*, PLOS ONE, 10 (2015), <https://doi.org/10.1371/journal.pone.0136497>.
- [23] B. D. MCKAY AND N. C. WORMALD, *Uniform generation of random regular graphs of moderate degree*, Journal of Algorithms, 11 (1990), pp. 52–67.
- [24] M. MOLLOY AND B. REED, *A critical point for random graphs with a given degree sequence*, Random Structures & Algorithms, 6 (1995), pp. 161–180.
- [25] M. MOLLOY AND B. REED, *The size of the giant component of a random graph with a given degree sequence*, Combinatorics, Probability, and Computing, 7 (1998), pp. 295–305.
- [26] M. E. J. NEWMAN, *Modularity and community structure in networks*, Proceedings of the National Academy of Sciences, 103 (2006), pp. 8577–8582.
- [27] M. E. J. NEWMAN, *Equivalence between modularity optimization and maximum likelihood methods for community detection*, Phys. Rev. E, 94 (2016), p. 052315, <https://doi.org/10.1103/PhysRevE.94.052315>.
- [28] M. E. J. NEWMAN AND M. GIRVAN, *Finding and evaluating community structure in networks*, Phys. Rev. E, 69 (2004), p. 026113, <https://doi.org/10.1103/PhysRevE.69.026113>.
- [29] M. E. J. NEWMAN, S. H. STROGATZ, AND D. J. WATTS, *Random graphs with arbitrary degree distributions and their applications*, Physical Review E, 64 (2001), p. 17.
- [30] J. REICHARDT AND S. BORNHOLDT, *Statistical mechanics of community detection*, Physical Review E, 74 (2006), p. 016110.
- [31] J. SJÖSTRAND, *Making multigraphs simple by a sequence of double edge swaps*, arXiv:1904.06999, (2019), pp. 1–11, <http://arxiv.org/abs/1904.06999>.
- [32] J. STEHLÉ, N. VOIRIN, A. BARRAT, C. CATTUTO, L. ISELLA, J.-F. PINTON, M. QUAGGIOTTO, W. V. DEN BROECK, C. RÉGIS, B. LINA, AND P. VANHEMS, *High-resolution measurements of face-to-face contact patterns in a primary school*, PLoS ONE, 6 (2011), p. e23176, <https://doi.org/10.1371/journal.pone.0023176>, <https://doi.org/10.1371/journal.pone.0023176>.
- [33] J. STEHLÉ, N. VOIRIN, A. BARRAT, C. CATTUTO, L. ISELLA, J. F. PINTON, M. QUAGGIOTTO, W. VAN DEN BROECK, C. RÉGIS, B. LINA, AND P. VANHEMS, *High-resolution measurements of face-to-face contact patterns in a primary school*, PLoS ONE, 6 (2011), pp. 1–13.
- [34] G. STRONA, D. NAPPO, F. BOCCACCI, S. FATTORINI, AND J. SAN-MIGUEL-AYANZ, *A fast and unbiased procedure to randomize ecological binary matrices with fixed row and column totals*, Nature communications, 5 (2014), p. 4114.
- [35] N. D. VERHELST, *An efficient mcmc algorithm to sample binary matrices with fixed marginals*, Psychometrika, 73 (2008), p. 705.
- [36] F. VIGER AND M. LATAPY, *Efficient and simple generation of random simple connected graphs with prescribed degree sequence*, in International Computing and Combinatorics Conference, Springer, 2005, pp. 440–449.
- [37] X. ZHANG AND M. E. J. NEWMAN, *Multisway spectral community detection in networks*, Phys. Rev. E, 92 (2015), p. 052808, <https://doi.org/10.1103/PhysRevE.92.052808>.